DOI https://doi.org/10.30898/1684-1719.2020.7.15
UDC 621.391.822

PHYSICS OF FLICKER NOISE AND MODIFICATION OF THE TRANSISTOR MODEL

A. S. Matsaev

The paper is received on July 22, 2020

Abstract. The article reveals the physical nature of flicker noise for electronic amplifiers. Experimental examples of the study of flicker noises are given with justification of the necessary and sufficient conditions for their existence, technical methods of regulation, forecasting, diagnostics and methods of their numerical assessment are determined. In order to reveal the physical essence and create a mathematical model of flicker noise for their numerical assessment, the Ebers-Mole model and the transport model of a bipolar transistor have been modified.

Keywords: flicker noise, 1/f noise, fluctuation noise, pink noise, excess noise, low frequency noise, thermal noise, shot noise, nonlinearity, drift, offset, zero component.

1. Physics of the flicker-noise

By definition [1, 2, 3], the flicker noise (aka: 1/f noise, fluctuation noise, pink noise, flickering noise, excessive noise, low-frequency noise, flickering noise) is a random signal whose spectral tension density is usually described by the formula:

$$S_f(f) = k/f^{\gamma} \quad (1)$$

Where f -is frequency, k -is a sized constant ($V/Hz^{1/2}$), γ -is a size less constant, which in most cases is close to a unit.

In 1925, J. B. Johnson first discovered and described the flicker noise, but its physical essence is still considered uncertain [1, pages 188-192]. This has been confirmed since 1968 at numerous (every two years) international noise and fluctuations conferences (ICNF). The last, 25th ICNF-2019 conference was held in Neuchatel, Switzerland, from June 18 to June 21, 2019.

In the article [5], we gave information about the typical level of equivalent input noise. We had developed several series of galvanic power amplifier chips, and noted the complete absence of flicker noises. The very fact of such a phenomenon obliges us to understand the reason for the absence of flicker noises and, if possible, to determine their physical essence, technical methods of control, regulation and guaranteed rationing in the construction of amplification Devices. For further proceedings, we found it convenient to use the electric amplifier scheme "100W" (see Fig.1), kindly provided by the US firm Linear Technology for free use and analysis. This electrical scheme is good because it is fully consistent with the classic methods of building amplifying devices, and each node in it is clear and well analyzed, for example in [7 - 10], except, the source of active displacement used in it on the V3 element, however, and it is clear and logical. The electric pattern of Fig.1 differs from the original by reducing the voltage gain to one, as in my power amplifiers [5], which simplifies and makes the presentation of the material more correct.

LTspiceXVII of the American corporation Linear Technology is used to analyze electrical values and characteristics, including noises. This allows you to eliminate inaccuracies and errors in the method of assessing physical values and processes, which is especially important for the correct assessment of noise. The chosen tool LTspiceXVII differs from others in that it is adapted to the most analog technology and allows you to get the necessary information with the accuracy of E-12 in typical use, and in the mode of refined analysis, up to E-18 and above. In particular, noise analysis is carried out taking into account the noise contribution of all elements of the electric scheme of medium integration, including the contribution of electrical connections. The choice of LTspiceXVII technical tool is additionally convenient because it will allow me to test my experimental and calculated results without significant resource costs.

Fig. 2 provides a graph of the equivalent input noise of the amplifier "100W", here is very clearly visible flicker noises, in general typical for many amplifiers. The latter circumstance will help to investigate the physics of flicker-noise in electronic voltage and power amplifiers.

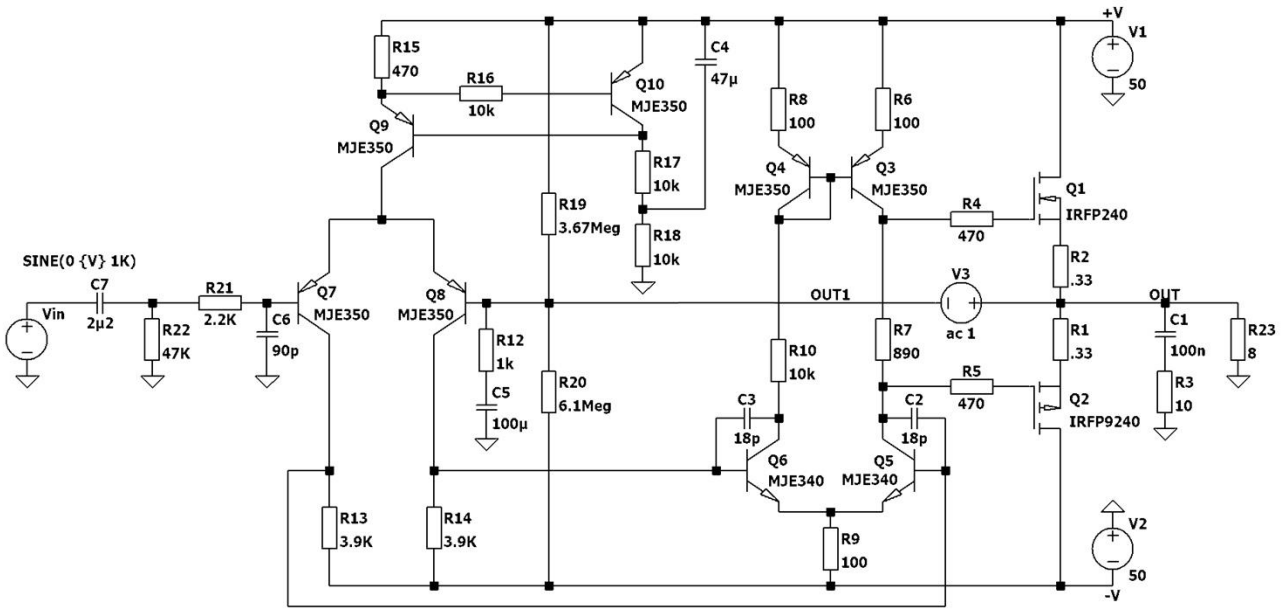

Fig. 1. Linear Technology's “100W” power amplifier.

When choosing to analyze the amplifier "100W" we noticed that the amplifier can easily be converted into a galvanic amplifier, amplifying signals starting from zero hertz, that is, constant signal voltages, as in all my galvanic developments power amplifiers. This is due to the use in the "100W" of the input differential amplifier on transistors of the Q7 and Q8 (including its auxiliary devices on transistors of the Q3-Q6 and Q9, Q10), which continuously compares the input voltage with the voltage of the load, while shifting the load The working point of the input amplifier is formed by an active source of V3 voltage. To convert the "100W" amplifier into a galvanic amplifier, I'll call it "100WG," it's enough to replace the C5 and C7 jumper, as shown in the Fig. 3.

The new galvanic amplifier "100WG" retains or remains close to the main characteristics of ARF, FChH, THD, powerful and dynamic characteristics. Once again, we will analyze the equivalent input noise for the galvanic amplifier "100WG" and as a result we will get a graph presented on the Fig. 4.

There is no flicker-noise in the "100WG" amplifier. It should also be noted that all the previously developed galvanic power amplifiers I have developed, for example in the work of the [5], in the case of installation between the signal source and the separation tank amplifier, acquire intense flicker-noises.

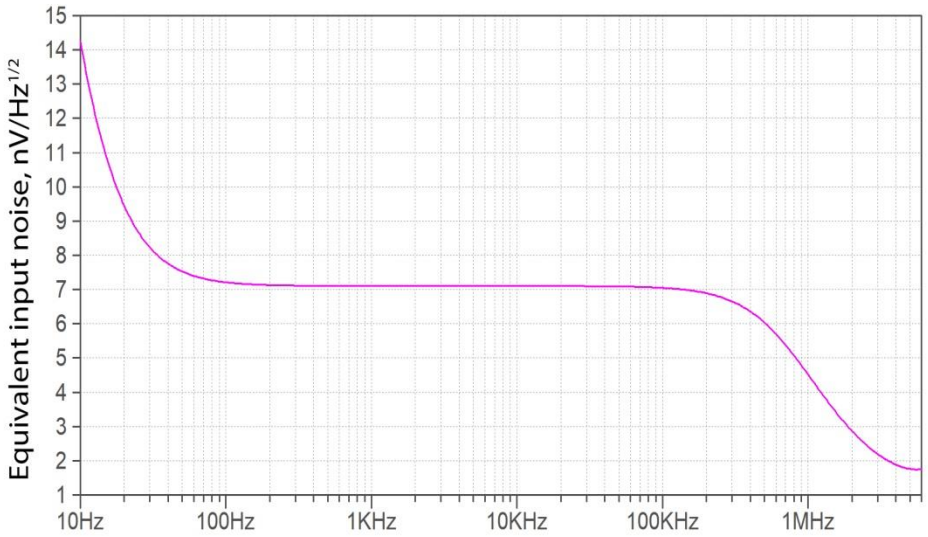

Fig .2. The graph of the equivalent input noise of the "100W" amplifier.

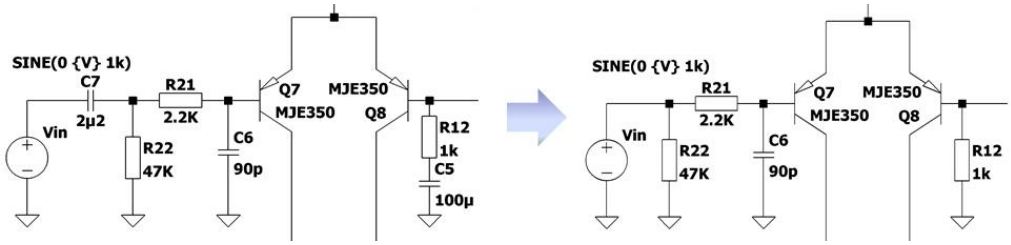

Fig. 3. Converting the “100W” amplifier into a galvanic “100WG” amplifier.

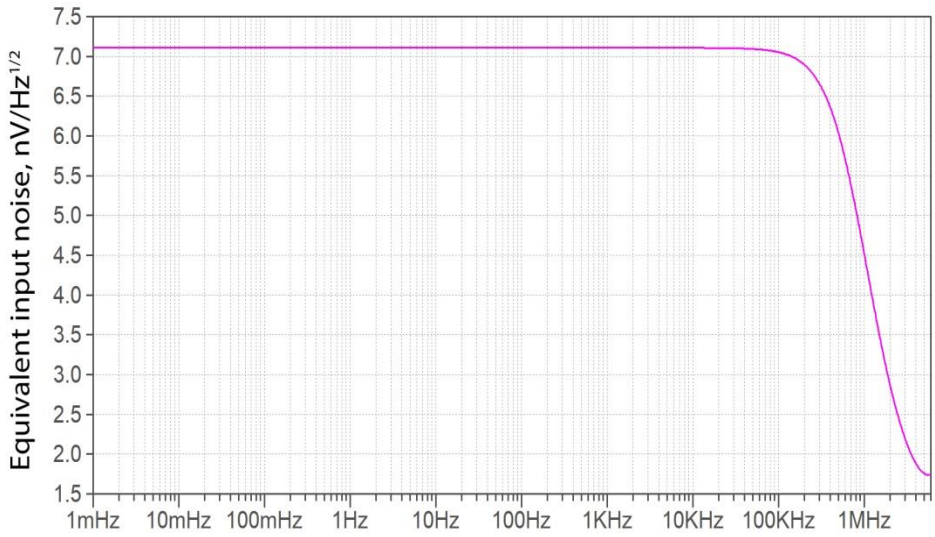

Fig. 4. The graph of the equivalent input noise of the “100WG” amplifier.

The fact of getting rid of flicker-noise is obvious, and now more research is needed. I think it is necessary to clarify that the linear dynamic voltage range of the amplifiers "100W" and "100WG" in my version of their use with a single voltage gain is 81.0V, and it corresponds to the dynamic range 38.26 mV voltage emitter-base U_{BE} transistor transition Q7, as shown in Fig. 5.

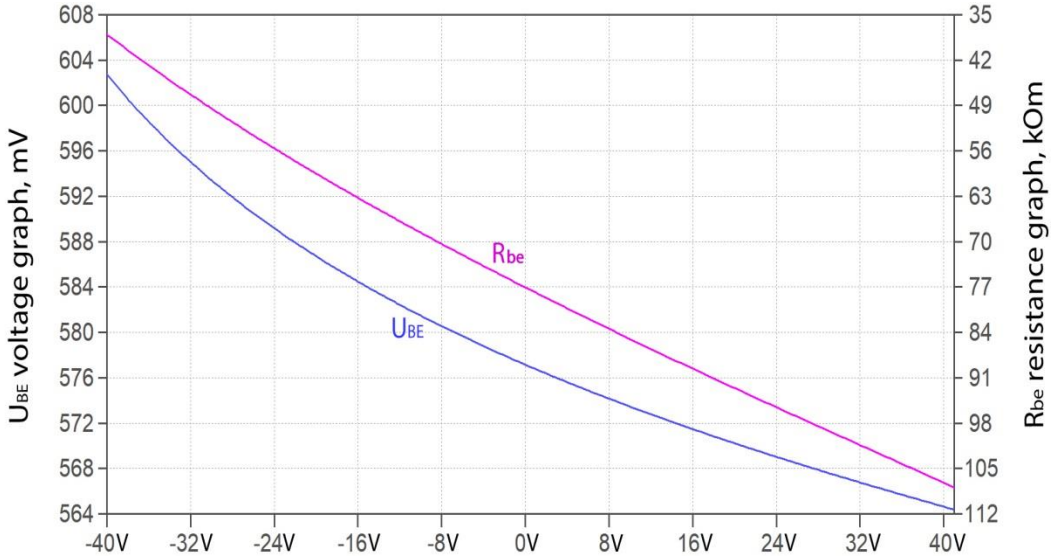

Fig. 5. U_{BE} and Rb dependency schedule from input amplifier voltage.

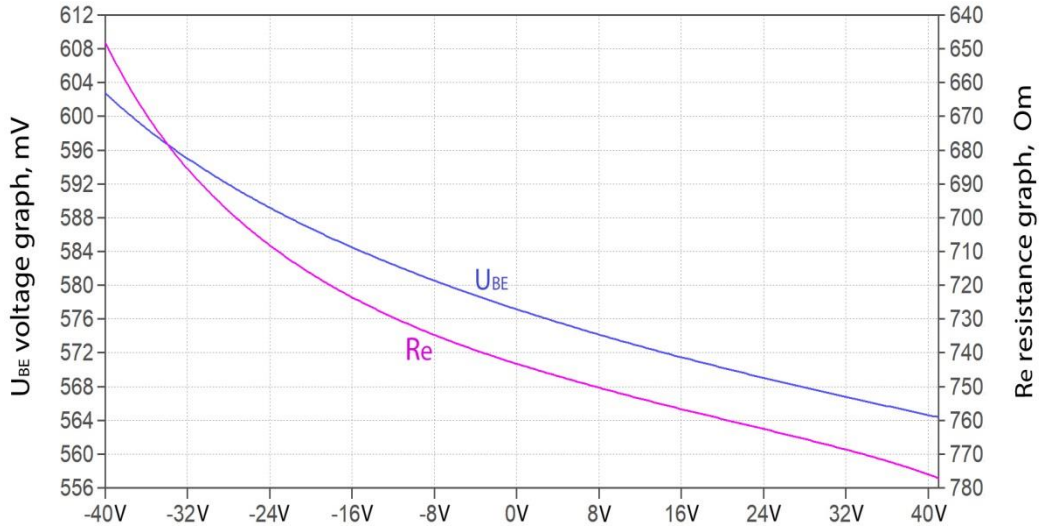

Fig. 6. U_{BE} and Re dependency schedule from input amplifier voltage.

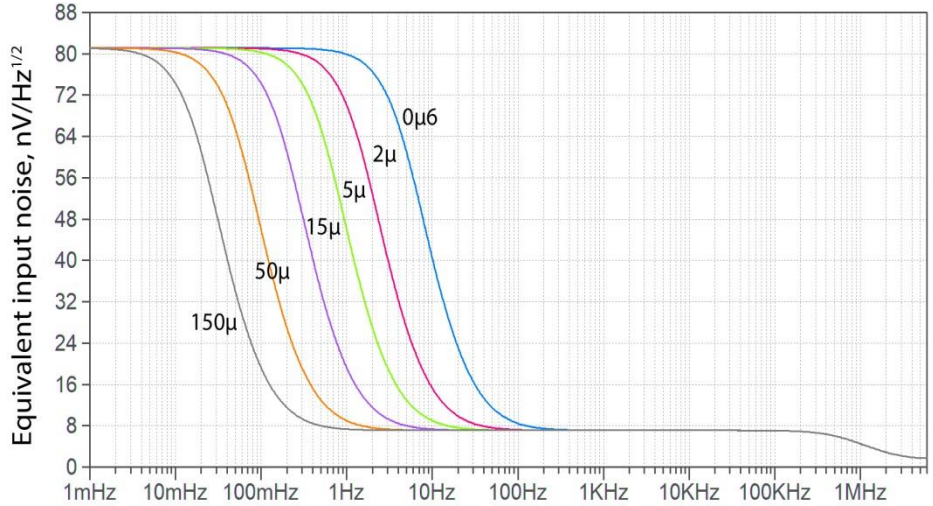

Fig. 7. Chart of the equivalent input noise of the "100W" amplifier for different C7 values.

The zero input corresponds to the U_{BE}=577.15mV shifting the working point of the transistor. On the right, the same graph shows the scale of values for R_{be} internal resistance graph. The zero input or the level of its own noise corresponds to the resistance of R_{be}=77kΩ. The following graphs of Fig.6, similar to Fig.5, show the scale of R_e emitter transition internal resistance values on the right. The zero input or the level of its own noise corresponds to the resistance of the R_e=743.77 Ω. We think it is necessary to note that the transistor Q7 is used in the signal shoulder differential amplifier and is powered by the current stabilizer included in the emitter chain. This explains the significant increase (on the stabilization rate) of the baseline and emitter resistance of the transistor in comparison with its reference characteristics. Numerical values will be useful further to assess the compliance of mathematical approximation with instrumental results.

Expand the range of measurement of equivalent input noise to low frequencies starting at 0.001 Hz and start by analyzing multiple graphs (see Fig.7) of the equivalent entry noise of the "100W" amplifier for the conditions of application of different denominations of capacity C7 capacitor.

On the right side of the chart you can observe the total thermal and fractional noise - white noise (with an intensity of 7.1 nV/Hz$^{1/2}$). There is a flicker-noise on the left side of the chart. Such a configuration of flicker-noise with a flat top has been repeatedly presented previously on the results of studies of different authors [1, Fig.2.5 Page.44; Fig.5.5 Page.131; Fig.6.1 Page.161].

For further presentation of the material, it is convenient to present our understanding of physics and the causes of flicker-noise.

Our judgment on the physical nature of the flicker-noise is based on the fact that on the nonlinearity of the transistor's non-basic transition Q7, any signals, including thermal and fractional noises, are distorted with an additional zero release in their spectrum component. The zero components induced from non-linearity is integrated, accumulated on the C7 dividing container and held on it for the duration of the R22, C7 chain integration. The potential accumulated on the C7 leads to an additional positive shift of the emitter-base transition, which in turn leads to an

increase in the permanent component of the basic and, accordingly, the collector current of the transistor Q7 and the proportional increase in amplification. As a result, there is an enhanced ultra-low frequency noise signal - flicker-noise, with all manifestations of random magnitude, because it is a derivative of random thermal and fractional noise.

The same can be said differently. The noise brought to the entrance of the amplifier is separated by the emitting-basic transition of the transistor Q7 from the cumulative noise generator, the transistor collector Q7, and all subsequent noisy elements of the electrical circuit, up to the R23 power load. From the cumulative noise generator, the noise energy through the emitter-base transition and the passive R21 divider, the R22 gets to the C7 capacitor. This chain is essentially an analog detector. The C7 capacitor accumulates a constant or zero components from the noise detector acting on the analogue detector. The level of accumulated zero component is determined and changed according to the energy of the cumulative noise generator; it is an integral derivative of thermal and fractional noise, which is the flicker-noise.

On Fig.7 the level of flicker-noise is almost ten times higher than the level of heat and fractional noises generated by it. The top flat area in the flicker-noise configuration is due to the fact that it is formed as a derivative of heat and fractional noise (see further (6) and (7)). The energy of thermal and fractional noises, though random, still has its limits characteristic of white noise, which is reflected in their integral derivative size - flicker-noise.

To form a flat flicker-noise area, it is necessary and sufficient to allow the phase shift on the C7 capacitor to be close to 0^O at the appropriate ultra-low frequencies of the range being analyzed. Inside the phase shift interval of 0^O - 90^O, there is a non-linear change in the level of flicker-noise from the maximum value to the level of thermal and fractional white-noise. Finally, there is no flicker-noise in the area where the Phase Shift of the C7 Jet Element is close or 90^O. It is impossible to accumulate integral accumulation of dynamic constant component of thermal and fractional noises, because the C7 reactive resistance at these frequencies is too small,

the phase shift is close to 90^{O}, the accumulation of asymmetric charge on the capacitor linings.

For visibility and a better understanding of physical processes, I find it useful to consider Fig.8. This shows a family of graphs on the emitter-basic transition from the input sinusoidal signal to the linear part of the dynamic range of the "100WG" amplifier with a 1/10 maximum signal level increase. The level of thermal and fractional noises at the emitter-basic transition of the transistor is certainly disproportionately small in comparison with the presented level of nominal sinusoidal signals, but Fig.8 very well represent the nonlinearity of the emitter-basic transition, and this non-linearity always remains an objective reality and the physical essence of semiconductor transition, both for small and large signals.

Charts on Fig.8 are expected, according to the known non-linearity of the emitter-base transition. If we consider each graph separately, it will be difficult to notice that the negative and positive half-wave, initially symmetrical signal, received different increments, the upper relative to zero half-wave stretched, and the bottom narrowed. The analysis of the family of graphs clearly demonstrates the nonlinearity of the emitter-basic transition of the transistor.

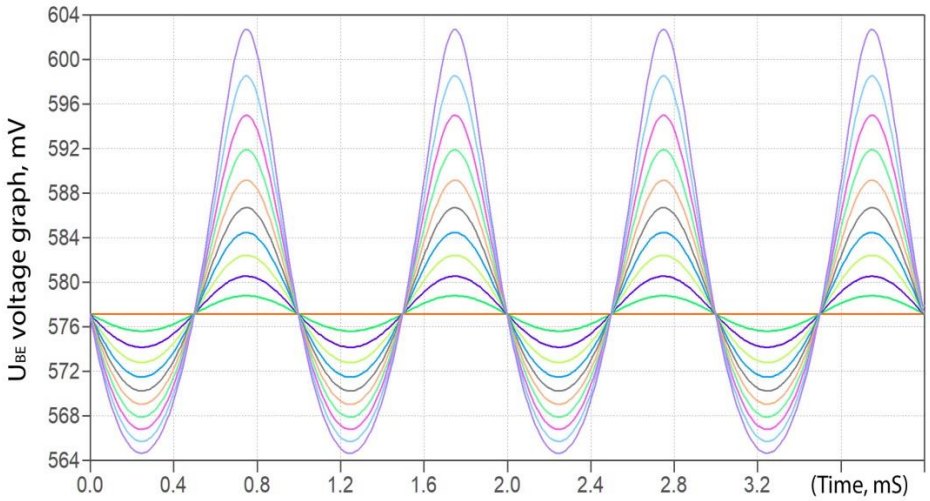

Fig.8. The family of waveforms on the emitter-basic transition of the transistor is Q7 without C7.

The “100WG” amplifier does not have a C7 dividing capacitor, and if you re-install it, you get a different family of graphs on the Fig.9. The C7 capacitor now

accumulates an integral accumulation of non-linear signal symmetry; the C7 capacitor is charged and shifts the transistor's working point by 16.23 mV.

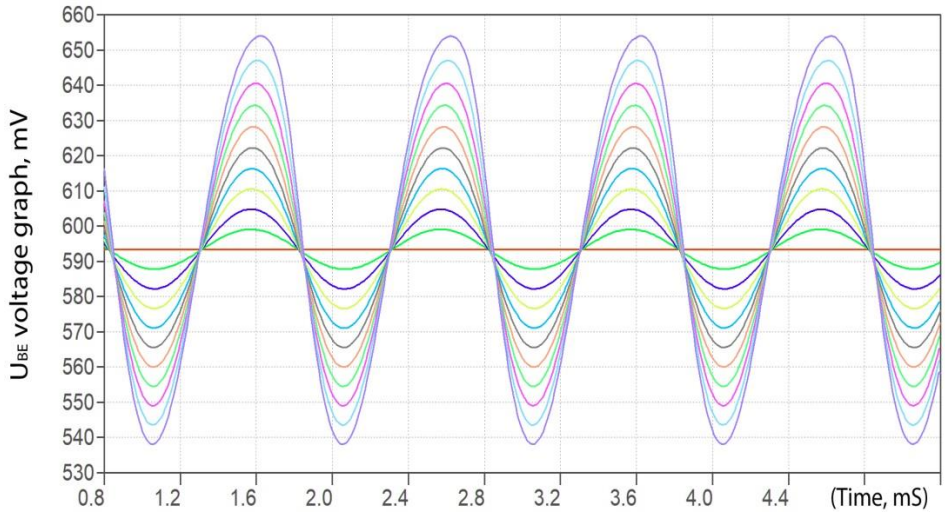

Fig. 9. The family of waveforms on the emitter-basic transition of the transistor Q7 with the included capacitor C7.

In this example, for the purpose of visibility of the process, the effects of the accumulation of a constant charge by the lining of the capacitor when exposed to a large sinusoidal signal are demonstrated. The noise signal will also continuously charge the C7 dividing capacitor with varying noise intensity and shift the transistor's working point with noise. This results in a flicker-noise.

In other words, the impact on a non-linear element by any signal results in the work point drift controlled by adding its zero components to the electrical power of constant displacement. In the event that the non-linear element, in addition to the electric propulsion force of constant displacement, is affected only by thermal and fractional noises, the noise generated by them is a flicker-noise.

Then we turn to the mathematical approximation of the physical essence of flicker-noise.

2. Modification of the Ebers-Moll model and the transport model of the bipolar transistor

For the normal mode of use of the transistor [7, page 78-81], with the $U_{BC} < O$, shifted collection-base crossing, the Ebers-Moll transistor model and the transport

model [9] have the same current expressions, as in this case both models do not take into account the currents of leakage:

$$I_B = \frac{I_S}{B_N} \exp\frac{U_{BE}}{U_T} \quad ; \tag{2.1}$$

$$I_C = I_S \exp\frac{U_{BE}}{U_T} \quad ; \tag{2.2}$$

$$I_E = I_S\left(1 + \frac{1}{B_N}\right) \exp\frac{U_{BE}}{U_T} \tag{2.3}$$

where I_B -is the current base; I_S - current collector; I_E - current emitter; I_S - saturation current (6,016-10^{-12}A, for MJE350 transistor); B_N - the rate of amplification by the normal mode ($B_N \approx 50 \ldots 500$, and for the transistor MJE350, - 100); U_{BE} - voltage displacement at the emitter crossing (for transistor Q7, in the amplifier "100W" and its modifications, - U_{BE} = 577.15 mV); $U_T = kT/\boldsymbol{e}_o$ - thermal potential (for silicon at a normal temperature of $U_T \approx 25.3$mV (10, page 87);

k - Boltzmann's constant; T - absolute temperature; $\boldsymbol{e}_o$ - electron charge.

Let the electromotive force of the displacement of the operating point of the transistor Q7 provides the constant component of the I_D displacement current, and the electromotive force of the signal represents the variable component and, accordingly, induces the variable component on the emitter-base junction $U_S \cdot \sin \omega t$.

To simplify, then we will assume that the initial phase is zero. In this case, the transistor's emitter-base transition will be at the total voltage of $U_{BE} = U_D + U_S \cdot \sin\omega t$. For example, the expression (2.1) in this case can be rewritten as:

$$I_B = \frac{I_S}{B_N} \exp\frac{U_D}{U_T} \exp\frac{U_S \cdot \sin \omega t}{U_T} \tag{3}$$

Decomposition $\exp\frac{U_S \cdot \sin \omega t}{U_T}$ in a sedate row of [11, page 115] gives:

$$\exp\frac{U_S \cdot \sin \omega t}{U_T} = 1 + \frac{U_S \cdot \sin \omega t}{U_T \cdot 1!} + \frac{U_S^2 \cdot \sin^2 \omega t}{U_T^2 \cdot 2!} + \frac{U_S^3 \cdot \sin^3 \omega t}{U_T^3 \cdot 3!} + \ldots + \frac{U_S^n \cdot \sin^n \omega t}{U_T^n \cdot n!} + \tag{4}$$

From the expression of the sedate function of $\sin^n x$ is known to [12, page 190], that the permanent component:

$$\frac{1}{2^{2n}} C_{2n}^{n} = \frac{1}{2^n \cdot n!} \tag{5}$$

has only even degrees of function. After substitution (5) in (4) there is an original, not previously found in the works of other authors, the expression of displacement of the permanent component of the semiconductor transition, taking into account the drift from the impact on nonlinearity of the signal or noise:

$$\xi = 1 + \frac{\Psi^2}{(2!)^2 \cdot 2^2} + \frac{\Psi^4}{(4!)^2 \cdot 2^4} + \frac{\Psi^6}{(6!)^2 \cdot 2^6} + \ldots + \frac{\Psi^{2m}}{((2m)!)^2 \cdot 2^{2m}} + \ldots = \sum_{m=0}^{\infty} \frac{\Psi^{2m}}{((2m)!)^2 \cdot 2^{2m}} \tag{6}$$

where: $\Psi = \frac{U_S}{U_T}$.

A modified dynamic transport model or Ebers-Moll model, for the normal (U_{BC} < O) mode of using a transistor, taking into account the drift components from the impact on the nonlinearity of the signal or own noise can now is recorded as:

$$I_{|B|} = \xi \frac{I_S}{B_N} \exp \frac{U_D}{U_T}; \tag{7.1}$$

$$I_{|C|} = \xi I_S \exp \frac{U_D}{U_T}; \tag{7.2}$$

$$I_{|E|} = \xi I_S \left(1 + \frac{1}{B_N}\right) \exp \frac{U_D}{U_T} \tag{7.3}$$

Previously [13], we had to get and use this expression with distinction in that only the Ebers-Moll model was used as the original mathematical model of the semiconductor transition of the bipolar low-power transistor. In that work, the expression (6/ helped to obtain a simple and extremely useful dependence of $\boldsymbol{\alpha \geq k}$ for the condition of compliance with the stability of the Raus-Hurwitz criterion in low-power amplifiers with deep positive feedback, where **α** is the stabilization factor the permanent component of the transistor's collector current; **k** - signal regeneration factor. The results of this ratio were fully confirmed experimentally in a wide range of temperature, constructive and other destabilizing factors.

The physical essence of constant drift in different semiconductor devices is similar and can be analyzed using a staid series /6/ and /8/. Degree row /8/ includes

only dynamic drift components, without taking into account static bias:

$$\Delta\xi = \xi - 1 = \frac{\Psi^2}{(2!)^2\cdot 2^2} + \frac{\Psi^4}{(4!)^2\cdot 2^4} + \frac{\Psi^6}{(6!)^2\cdot 2^6} + \ldots + \frac{\Psi^{2m}}{((2m)!)^2\cdot 2^2} + \ldots = \sum_{m=1}^{\infty} \frac{\Psi^{2m}}{((2m)!)^2\cdot 2^{2m}} \quad (8)$$

Full expressions of the dependence of dynamic drift constant component of transistor's ducts from the impact of the signal or internal noise take the form:

$$\Delta I_{|B|} = (\xi - 1)\,\frac{I_S}{B_N}\exp\frac{U_D}{U_T} \quad (9.1)$$

$$\Delta I_{|C|} = (\xi - 1)\,I_S \exp\frac{U_D}{U_T} \quad ; \quad (9.2)$$

$$\Delta I_{|E|} = (\xi - 1)\,I_S\left(1 + \frac{1}{B_N}\right)\exp\frac{U_D}{U_T} \quad (9.3)$$

On the Fig.10 the equivalent diagram of the amplifier's input chains is "100WZ" taking into account the internal structure of the transistor in accordance with the [7, page 78-81], [14, page 162, Fig.15], (7.1 – 7.3).

Before it moves to the numerical calculation of drift of the constant component of shifting the working point of the transistor Q7 from the allocation on its non-linearity of zero components of thermal and fractional noises, we will make the following observation. The transistor Q7 is used in the signal shoulder differential amplifier and is powered by an electric stabilizer included in the emitter chain. This explains the significant increase (on the stabilization rate) of the baseline and emitter resistance of the transistor in comparison with its reference characteristics.

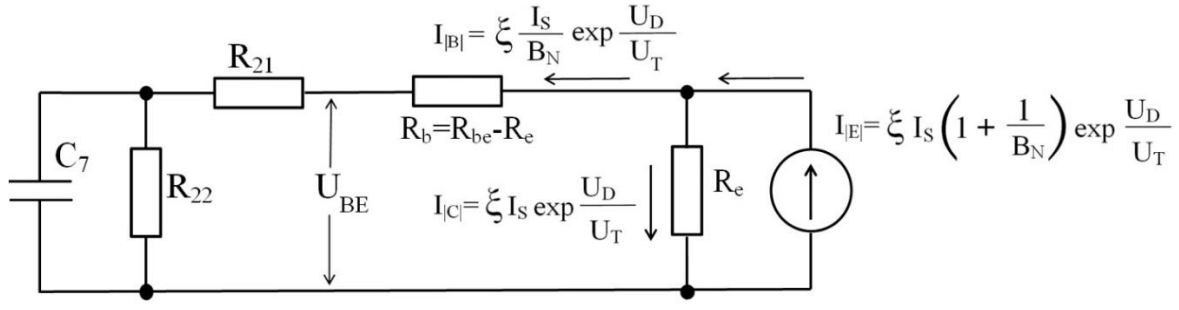

Fig. 10. The equivalent scheme of the "100W" amplifier input chains.

Next,weI use the expression of Nikvist [14,Ch.2,(90)], [15, (3.11)], [16], [17] to determine the equivalent, current noise level. As a result, I will receive the

expression Ψ for experimentally measured total thermal and fractional noise, in the ΔF range of the ARF amplifier:

$$\Psi = \frac{U_N \cdot (\Delta F)^{1/2}}{U_T} \qquad (10)$$

Now, using the expression /9.1/, I will get an increment of flicker noise from the non-linear emitting-base transition of the transistor Q7 and integrated on the reactivity of C7, zero component, derivative of thermal and fractional noise, taking into account the bypass elements of R22, R21 input chains of the amplifier "100WZ":

$$\Delta U_{FN} = \Delta I_{|B|} \cdot R_{be} \cdot (R_{22} + R_{21}) / (R_{be} + R_{22} + R_{21}) = 71{,}6 \text{ nV} \qquad (11)$$

where: R_{be} = 77,0 kΩ; $I_S = 6{,}016 \cdot 10^{-12}$A; B_N = 100; U_D= 577,15 mV; U_T = 25,3mV; R_{22} = 47 kΩ; R_{21} = 2,2 kΩ; U_N=7,1 nV/Hz$^{1/2}$; ΔF=1,0 MHz.

The flicker noise level on the flat section will be:

$$U_{FN} = \Delta U_{FN} + U_N = 78{,}7 \text{ nV/Hz}^{1/2} \qquad (12)$$

The result is fully consistent with the experimental schedule of flicker noise on Fig.7.

The modified Ebers-Moll mathematical model and the modified transport mathematical model of the transistor confirm my assertion that the physical essence of the flicker noise is that the nonlinearity of the transistor's emitter transition is Q7 any signals, including thermal and fractional noises are distorted with the release in its spectrum of an additional zero component. The zero components induced from non-linearity is integrated, accumulated on the C7 dividing container and held on it for the duration of the integration of the R22, C7 chain. The potential accumulated on the C7 leads to an additional positive shift of the emitter-basic transition, which in turn leads to an increase in the permanent component of the base and, accordingly, collector's current.

As a result, there is an enhanced ultra-low frequency noise signal – flicker noise, with all manifestations of random magnitude, because it is a derivative of random thermal and fractional noise.

The resulting modified Ebers-Moll mathematical model and the modified transport mathematical model of the transistor accurately correspond to the physical processes of normal transistor use, with the transistor back shifted U_{BC} < O collection-base transition, in the mode of small signals and noises.

For large signals, in the entire linear dynamic amplifier range, the resulting modified mathematical model significantly improves compliance with physical processes and near-describes the drift of the transistor's work point from zero component of the affective signal. A further modification will be required to more accurately match, in particular to take into account the dependence of the B_N gain factor change from the level affecting the signal transistor. The need for this correction is demonstrated by the experimental graph BN Transistor Q7, in the dynamic range of the amplifier "100WZ" that is shown in the Fig.11.

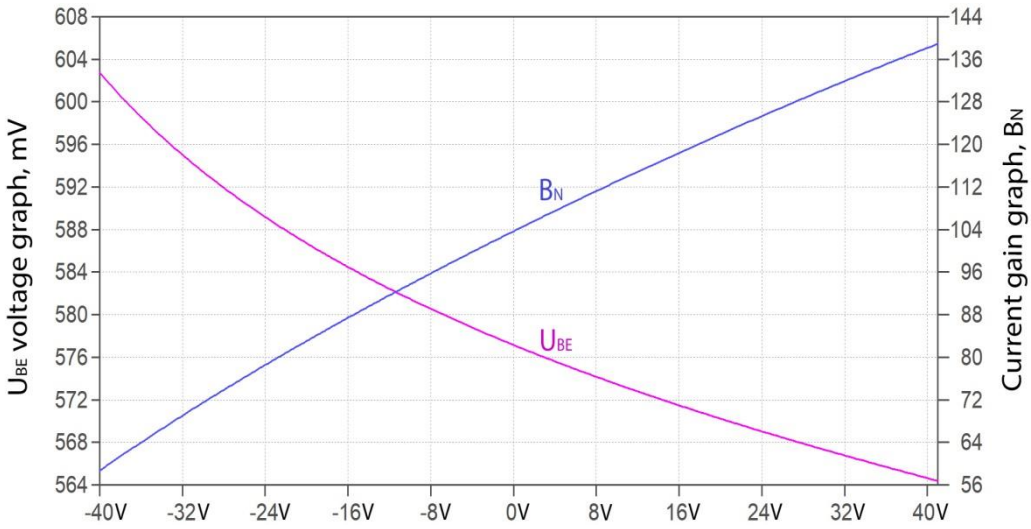

Fig.11. B_N transistor Q7 amplification chart, in the dynamic range of the “100WG” amplifier.

References

1. Buckingham M.J. *Noise in Electronic Devices and Systems*. John Wiley & Sons. 1985. 372 p. ISBN 013624453X, 9780136244530

2. Kogan Sh. M. Low-frequency current noise with a spectrum of type 1/f in solids. *Physics Uspekhi*. 1985. Vol.145. No.2. P.285-328.

https://doi.org/10.3367/UFNr.0145.198502d.0285

3. Weissman M.B. 1/F noise and other slow, no exponential kinetics in condensed matter. *Rev. Mod. Phys*. 1988. Vol.60. No.2. P. 537.

4. *Proceedings of 25th International Conference on Noise and Fluctuations – ICNF 2019* [online]. URL: https://icnf2019.epfl.ch/

5. Matsaev A.S. Comprehensive innovation in power amplifiers. Development of the first series of microcircuits. *Uspekhi sovremennoy radioelektroniki*.- *Advances in modern radio electronics*. 2019. No. 7. P.69-77. (In Russian)

6. LTspiceXVII library [online]. URL: https://www.analog.com/ru/design-center/design-tools-and-calculators/ltspice-simulator.html

7. Tietze U., Schenk C. Halbleiter-Schaltungtechnik. Springer. 1999. Vol. 1.

8. Tietze U., Schenk C. Halbleiter-Schaltungtechnik. Springer. 1999. Vol. 2.

9. Getreu I. *Modeling the Bipolar Transistor*. Amsterdam, Elsevier, 1978.

10. Horowitz P., Hill W. The *Art of Electronics*. Cambridge University Press. 1980. 1125 p. ISBN 5-03-002336-4.

11. Dwight H.R. *Tables of Integrals and Other Mathematical Data*. The Macmillan Company. 1961. ISBN-10 0023311703. ISBN-13 978-0023311703.

12. Brychkov Yu.A., Marichev O.I., Prudnikov A.P. *Tablitsy neopredelonnykh integralov* [Tables of indefinite integrals]. Moscow, Fizmatlit Publ. 2003. 200 p. (In Russian)

13. Matsaev A.S. Stabilization of amplifier characteristics with positive feedback. *Radiotekhnika – Radio Engineering*. 1994. No.6. (In Russian)

14. Sze S.M. *Physics of Semiconductor Devices*. John Wiley & Sons. 1981.

15. Zhigalsky G.P. Lecture course *"Fluktuatsii i shumy v fizicheskikh sistemakh"* ["Fluctuations and Noises in Physical Systems"]. Online resource. URL: https://studfiles.net/preview/331761/ (In Russian)

16. Van der Ziel A. *Noise in Measurements*. John Wiley & Sons, N.Y. 1976.

17. Van der Ziel A., Chenette C. H. Noise in Solid State Devices. *Advances in Electronics and Electron Physics*. 1978. Vol. 46.

For citation:
Matsaev A.S. Physics of flicker noise and modification of the transistor model. *Zhurnal Radioelektroniki - Journal of Radio Electronics*. 2020. No. 7. https://doi.org/10.30898/1684-1719.2020.7.15